Using a planar EIT as a Structural Health Monitoring method to detect and evaluate the damage to CFRP composite used in aerospace structures

Ali Zarafshani
School of Engineering and Informatics,
University of Sussex,
Brighton, UK
A.Zarafshani@sussex.ac.uk

Thomas Bach
Head of Research
Sensatech Research,
Brighton, UK
Tom@sensatech.com

Prof Chris Chatwin
School of Engineering and Informatics,
University of Sussex,
Brighton, UK
C.R.Chatwin@sussex.ac.uk

***Abstract*—Electrical Impedance Tomography (EIT) as an imaging technique producing a 2D or 3D impedance image (conductivity or impedivity) of the subject under test. It can be used for delamination detection and evaluating the damage location, size, strain and severity for Structure Health Monitoring (SHM) of aerospace composites i.e. Carbon-fibre-reinforced polymer (CFRP) composites.**

Keywords—Electrical Impedance Tomography, Structural Health Monitoring, Damage detection, CFRP

I. INTRODUCTION

Fibre-reinforced polymer (FRP) and glass fibre reinforced polymer (GFRP) structures are commonly used in the aerospace industry. In 1996 Sir Harry Kroto from University of Sussex with Richard Smally from Rice University were awarded a Nobel Prize in chemistry for discovering the C60 molecule [1], which was revolutionary for nanomaterials and led to the creation of carbon nanotubes and nanofibers. Carbon-fibre-reinforced polymer (CFRP) composite is another material used in aircraft structures. It is conductive due to the carbon fibres touching each other. Even lower conductivity is attained with glass fibre-reinforced polymers with nanocomposite matrices. An alternative method that also offers well controlled and lower conductivities is to coat molecules than are normally insulators with PolyPyrroles (PPy) [2]. Milliken Textiles perfected this process and made a range of conductive textiles that can be used as part of a FRP. Carbon composites and Carbon nanotubes (CNTs) with unique mechanical and electrical properties are being utilized to alter the electrical conductivity of polymers used in commercial and military aircraft bodies. These structures can be built using carbon composites such as CFRP containing FRP and CNTs. This can lead to weight reduction, greater stiffness, better fatigue characteristics, higher reliability and controlled higher electrical and thermal conductivity. These latter properties can be used to enable electromagnetic invisibility of the airplane.

The complexity of polymer composites creates a challenge for Structural Health Monitoring (SHM); i.e. detecting and assessing damage, damage growth rates and the effects of damage on the structure during inspection intervals. Thus tracking the condition of a structure is vital in Structure Health Monitoring (SHM). Traditionally SHM methods are based on different types of nanostructure sensors i.e. strain gages or piezoelectric transducers, fibre optic, or active or passive ultrasonic, or microwave transducers,.

Electrical Impedance Tomography (EIT) is a low-cost, safe imaging technique that indicates the characteristic of the subject under test. It has been used as a medical imaging technique by producing conductivity or permittivity images [3-5]. Similarly, in the case of SHM, conductivity images are produced to distinguish the condition of a structure by assessing the location, size, strain, and severity of damage. Typically the electrical conductivity data of the structure is established by injecting a known value of single or multi-frequency current points through the electrodes attached to the surface and measuring the potential differences over the subject under test with other electrodes attached to the surface.

There are numerous groups' that recently made use of conductivity images based on changes in electrical conductivity of semiconductor materials to assess damage [6-11]. In case of GFRP, Bryan Loyola [10] in his lab coated GFRP with CNT thin films and Tyler Tallman [6, 7] also laminated the GFRP with Carbon Black (CB) filler as a nanocomposite martial in order to produce conductivity images to detect the damage. In the case of CFRP, Schueler, Loyola and Fan [10, 12, 13] presented EIT systems to detect and assess the structural damage. Yet, most of the research is based on feasibility studies and focused on the martial composites and the possibility of using EIT as a SHM; this research presents an EIT device and our focus will be based on electrical challenges and experiments.

Existing Sussex-EIT systems designed for breast cancer detection where a saline solution tank is used as a homogenous conductive medium and the sensor pads are placed at the bottom of the tank to connect via the saline to the breast. We have redesigned the EIT system to make a suitable system capable of producing a conductance image of airframe materials. This paper describes the advantages of using a planar EIT sensor array as a new approach in SHM and focuses on the design of such a planar EIT system that shows conductive images for improved delamination and damage detection in both GFRP and CFRP.

II. METHODOLOGY

EIT is one of the new techniques that has been employed as a SHM technique based on comparing the differences of the distributed conductivity on the composite network to evaluate the structural condition. To fulfil the SHM requirements, we have designed a portable EIT system with a planar electrode plate to be attached to the structure for detecting damage structures, especially to the nanotube and nanofiber structures.

The most recent techniques for the EIT system are based on ring (or circular) electrode plate in which electrodes are connected to the edge of the subject. It has been used by many groups for clinical and industrial applications for screening relative conductivity of a medium where, for example in the case of monitoring of regional lung function or respiratory system the electrodes are placed in a ring around the chest, which is the subject under test [14-17].

In the case of EIT used for SHM, it would be quite challenging to design an EIT device which can be perfectly attached to the subject (e.g. carbon nanotubes) to produce 3D conductivity images. The ring topology electrode plate is not applicable for detection of the damage to the structure which is installed on the fuselage. In addition the sensitivity of the relative conductivity of the subject or detection in the ring topology decreases from the boundary to inner area since electrodes are located on the edge of the sample under test and the highest electrical field will be near the electrodes and it will be reduced as we move away from the electrodes. As a replacement for ring topology, a planar electrode plate (array of electrodes) can be attached to the structure (fuselage) where out of phase currents injected from any two electrodes and the complex voltages on the remaining pairs measured to obtain data that can be used to construct a 2D or 3D image with a penetration around 10mm and thus used for detecting damage and assessment of the structures.

The proposed electrode plate has 85 pads placed in a planar circular array of 180mm diameter with 17mm distance between each of the two pads that are pressed against the surface of the composite material to be examined with low resistance conductive conformable pads. Ideally a single system would be able to be used on materials of high and low conductivity.

III. RESEARCH PROTOTYPES TARGETING

The structure of the EIT is based on injecting a known value of current and measuring the voltage to evaluate the transfer impedances. The typical configuration used in EIT is to drive any two pads with constant currents 180-degree out of phase and to measure the difference voltage on any other pair of pads as shown in Fig. 1(a). This structure is implemented by allocating a current source and its mirror current source to two driven electrodes using multiplexers and by allocating the receiving electrodes with multiplexers as shown in Fig. 1(b), the overall block diagram of the multichannel EIT system. The voltages on the receiving electrodes is put to a high input impedance differential voltage amplifier. The image of the impedance profile of the material is found using the received data and an inverse mathematical procedure.

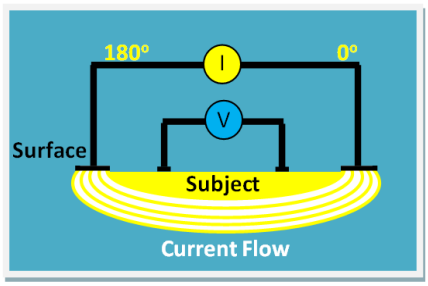

(a)

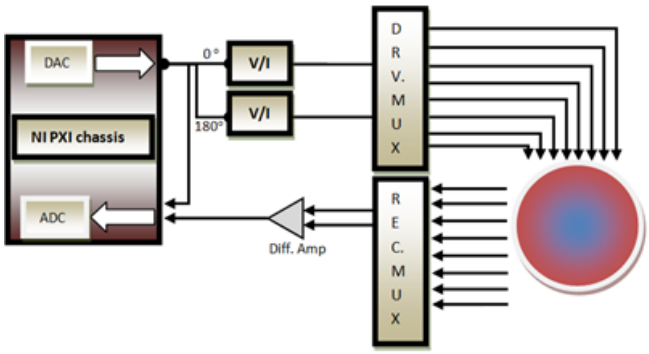

(b)

Fig. 1 (a) four electrode method, (b) block diagram of multi-channel EIT system

In order to be able to arrive at a good noise free inverse image we need to have good noise free data.. If we assume that the airframe is picking up voltage noise then this will be present on the two receiver pads. If we make the voltage greater on the drive pads by using a larger current this will mean that greater data voltage will be present on the receiver pads and thus the data SNR will be larger.

In order to determine the current necessary to drive the pads and keep the data SNR large enough we have used the hypothetical design rule that our injected current must be large enough to give us at 100mV peak to peak maximum on enough of the receiver pads for us to get a good inverse reconstruction. We assume that this will be met if 0.1 of the voltage on a pad transmitting current is greater than $100m^{V}$ peak to peak. Thus the minimum voltage on a driven pad is 1^{V} peak to peak.

In order to see what the range of resistances the driven pads can have, let us first examine what is the maximum current that we can deliver through the multiplexers (MUXs) before it clips the rail, or exceeds its heat dissipation limit or goes outside the recommended maximums specified in its data sheet.

As an example in the Sussex EIT system we used the ADG2128 [18], which is a 12×8 cross-point switch as a drive multiplexer (DRV-MUX) to select which pads were used to inject current. The ADG2128 has a maximum on-resistance of 35Ω. It is typically powered from $\pm5^{V}$ rails. The implications then of using $\pm5^{V}$ rails and having the R_{ON}=35Ω, are that the maximum value of current (the peak current amplitude) is limited to $\pm143m^{A}$ ($\pm5^{V}$ divided to 35Ω). The data sheet recommends a $25m^{A}$-$65m^{A}$ current limit for the ADG2128

multiplexer [18], therefore we have to set our design limit to $25m^A$. Limiting our current to $25m^A$ peak to peak means we can expect to see peaks of $\pm0.875^V$ across the on-resistance of 35Ω, switch effectively reducing the useable power rails to $\pm4.125^V$ ($\pm5^V$ minus $\pm0.875^V$).

In addition, in regard to the type of current source, for example for the case of the improved Howland current source [19], if it has a rail voltage of $\pm5^V$ but voltage is lost in the output series resistor even when the high speed operational amplifiers are used, it is not rail to rail output. These factors limit our output voltage to almost $\pm2^V$ (in case of $\pm5^V$), thus the multiplexer rail voltage is not the main limiting factor where $25m^A$ is delivered causing a 0.875^V drop across the multiplexer, furthermore the rail voltage of the op amp of the improved Howland current source limits the output voltage on the pad to $\pm1.125^V$ ($\pm2^V$ minus $\pm0.875^V$). Accordingly, with 25mA delivered this will be limited by the improved Howland current source, additionally voltage drop across the on-resistance of the multiplexer to a sensor pad with the contact resistance of 45Ω before clipping takes place in the current source. That means $R_{\_pad}$ which is equal to 2^V minus 0.875^V then divided by 25mA which the V_{pad} is equal to 1.125^V (equal to 25mA times 45Ω). Using these assumptions we will get a good inverse if 0.1 of the voltage on a pad transmitting current is greater than $100m^V$ peak to peak, we see that this is met since $0.1V_{pad}$ equal to 0.1125^V.

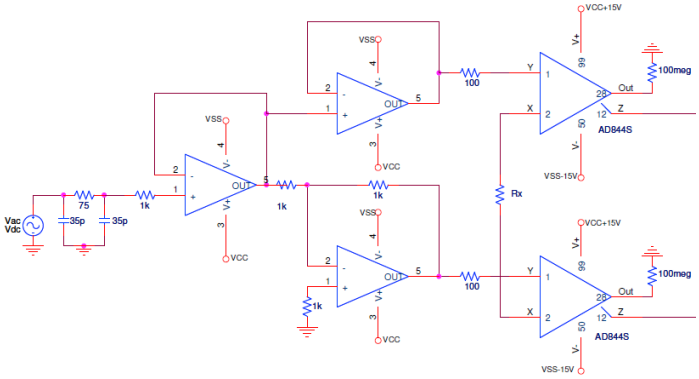

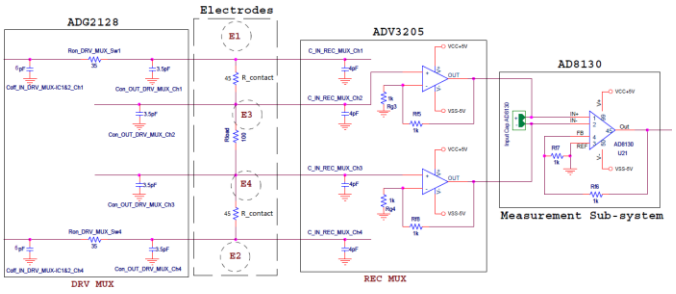

Fig. 2 Simulation block diagram of (a) current conveyor current source, (b) DRV&REC MUXs with four-electrodes (E1, E2, E3 & E4) and Measurement Sub-system of multi-channel EIT system consists of on-resistance of drive contact resistance

There is no maximum theoretical pad resistance caused by the above limitations as long as we can reduce the current delivered by reducing the voltage drive to the improved Howland current source. For example the output voltage limitation to $\pm2^V$ and the fact that we need 1^V on the driven pad means if our average pad resistance is 4kΩ, we can use this as long as we limit out current drive to 0.5mA. However the improved Howland current source has a finite output impedance that is in parallel with the load formed by the pad resistance. This limits and requires careful calibration if we desire to use a pad resistance near in value to this output impedance. Also internal capacitances to the power rails in the ADG2128 act to limit the upper frequency that can be used. As a conclusion, using the above assumptions, the 85-pad system can be used but the target material cannot have a bulk resistance that would make the resistance of a single 0.95mm sensor pad less than 45Ω.

In regard to the target airframe materials that have a large enough conductance to make the pad resistance less than this, a design of the system we will need to use multiplexers with reduced multiplexer on-resistance to be able to drive lower pad resistances if we improve our constant current source so it worked form larger power rails and used multiplexers with lower on-resistances. For example the MAX4601 has an on-resistance of 2.5Ω and power rails of $\pm20^V$ and the TS3A5223 has an on-resistance of 0.45Ω but with power rails limited to 0 to 3.6^V. However looking at a pad resistance of 1Ω we can see that since 1A would be delivered to obey our 1^V hypothetical rule that means the MAX4601 would be dissipating 2.5^W and the TS3A5223 $450m^W$. These would exceed the data sheet recommended maximum power dissipation of the MAX4601 which is $571m^W$ and the TS3A5223 which is $430m^W$. Thus for very low pad resistances we would need to use a current source powered with higher rail voltages and a drive multiplexers with lower on-resistances.

Using multiplexers and especially cross-point switches can greatly lower the component count and lower variation in measurement of different pads because it allows us to use the same block of circuit, such as a current source and a measurement subsystem, for different pads. This also allows us to have a built in calibration pad to check and correct for temperature and component drift. However, as we discussed above the on-resistance and power rails of the multiplexer affect our ability to inject enough current to get a good SNR with low pad resistances.

An industrial application of EIT systems for CFRP and GFRP composites could be based on applying a known value of current, amplitude between 25mA to 100mA that is injected into the subject and measuring the resulting potentials DC or AC frequencies around 100 Hz to a 10kHz in order to produce a conductivity image of the structure based on the four-electrode method as shown in Fig. 1(a). The Sussex 85 pad system used a standard EIT configuration of driving any two pads with a constant current and measuring the difference voltage on any other pair of pads. The electrode plate structure used is circular instead of square as previously designed by the Author and other existing EIT systems presented for SHM. This circular electrode plate will produce a uniform mesh area whereas a square electrode plate will produce an nonuniform

mesh and electrode field at the corners. The driven pads of this circular electrode plate were driven for our testing with an improved Howland current source or current conveyor current source based on AD844 [20] current conveyor module with power rails of $\pm 18^{V}$. The ADG2128 12×8 cross-point switch allowed us to drive the pads either singly or in pairs or as groups. The Sussex system allowed us drive the pads either with voltage or current to also measure the current or voltage of the driven pads. In order to decrease problems due to contact impedance or variability of on-resistance of any multiplexers used in series with the drive currents, we have chosen the most common configuration which is to drive a pair of pads with a 180 degree out of phase constant currents and to measure the voltage difference with a high input impedance difference voltage amplifier of AD8130 [21] on all other non-driven pairs as is utilized on the receiver multiplexer of ADV3205 [22] with a buffered cross point switch. For signal-to-noise reasons (improving Signal-to-Noise Ratio, SNR) we have chosen to use systems based upon AC current delivery and measurement of difference voltage by narrow band synchronous demodulation as shown in Fig. 1(b). The image is reconstructed by modifying "EIDORS" software [23, 24] based on 85 electrodes planar electrode plate with the refined mesh as shown in Fig. 3.

For initial calculations upon which we base our design, we assume that identical but 180-degree out of phase voltages exists on both of the current transmitting pads. This will not necessarily be the case but will be affected by where on the airframe the earths or capacitive earths are.

In regard to the EIT block diagram when the contact conductivity is low compared to the conductivity of the material we could use a signal generator and data acquisition system (DAQ) modules, which are set up on a National Instrumentation chasses (NI PXI modules) to create 14-bit arbitrary waveform generator and to receive the output voltage measurements. The input voltage signal is passed to a voltage-to-current conveyor that is based on the current conveyor which serves as a current source circuit. We used two stages of multiplexers to share the current source and a differential voltage amplifier between all electrodes as shown in Fig. 1(b). Using this system with the target materials where the resistance is from 50Ω to 1kΩ.

IV. Result and Discussion

The real problem in the design is that the contact conductivity is likely to be variable and with the same order as the conductivity of the material. This can cause changes in our measurements that can be interpreted as damage when the inverse is performed, on the other hand there can be surface damage that is sensed.

Therefore the contact conductivity needs to be maximized, so it is an order of magnitude lower than the magnitude of conductivity of the material or measured in order to eliminate these effects. Theoretically by using constant current injection we can overcome this problem but it requires the ability to deliver constant currents at high voltages when the contact impedance is high in order to inject the same current. An alternative approach is to use such high frequencies that the capacitive coupling becomes a major factor.

The electrical conductivity of carbon nanotube (CNTs) is very high up to 10^{7}S/m but the CFRP composite has very low electrical conductivity compare to CNTs. Thus we produced a mesh network with the same electrical conductivity as the composite then made a hole with different sizes in different locations inside and reproduced the mesh with this damage. Thus, we simulated a composite conductivity map and compared the conductivity images of the structure with/without a damaged structure composite. Afterward we try to change the electrical conductivity of the material using Monte Carlo analysis, which allows examination of the effects with 100 runs, with the Gaussian distribution and with 1536 as the random seed number based on error performance analysis. Finally we produced the conductivity images and assessed the performance of the system for detecting the damage to the structure.

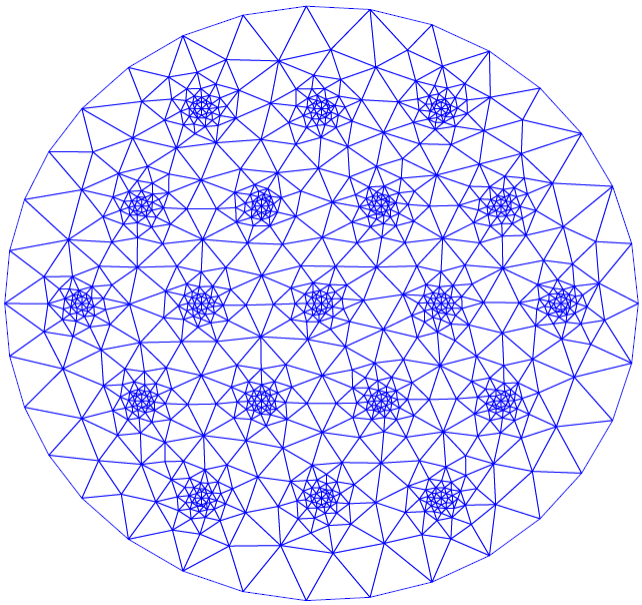

(a)

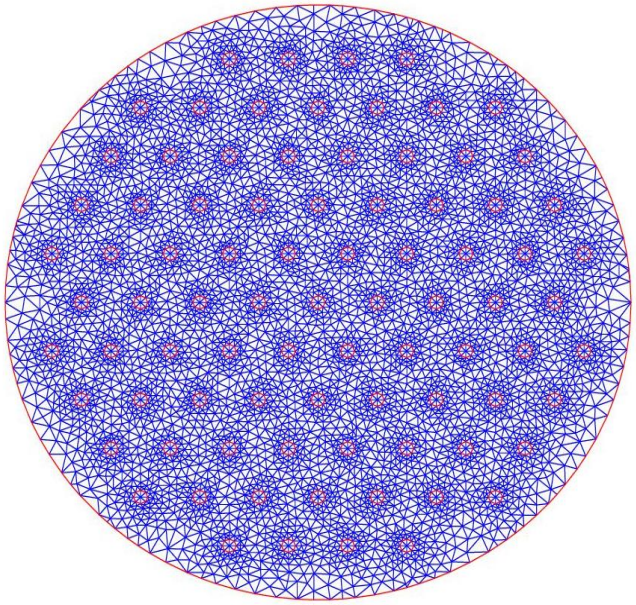

(b)

Fig. 3(a) shows Initial-Mesh of 19 electrodes of a measurement combination where two electrodes are injecting current with 12 voltage measurements (b) Refined-Mesh with location of 85 electrodes in a planar circular electrode plate

The planar electrode plate consists of 85 spring-loaded, stainless steel electrodes with gold plated tips and the tip style is a 7-points crown with a higher set middle point. Its internal resistance is less than 20mΩ (INGUN GKS-100 224 130A 2000E)as shown in Fig 4 (a) then these electrodes connected to the sliver loaded pads by pressed to the material which will help to reduce as small as possible interference of contact electrode. Fig 4(b) shows the EIT image reconstruction based on image reconstruction software and simulation data with impact of 100J force on the surface.

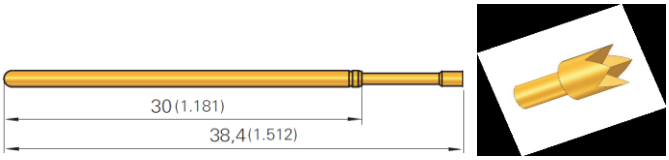

(a)

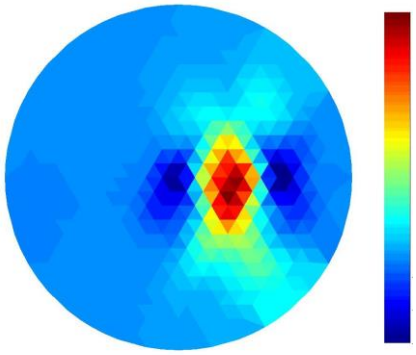

(b)

Fig. 4 (a) the planar electrode of spring-loaded stainless steel with flat style shape (b) EIT image reconstruction.

V. Conclusion

This paper presents EIT for damage detection as a health monitoring system for structures of CFRP and the possibility of using a thin film in case of GFRP. This study is based on a design of a planar EIT device to detect the damage, with different sizes and locations in the structure by producing a conductivity image of the materials that would be applicable in industrial aerospace applications.

VI. References

[1] H. W. Kroto, J. R. Heath, S. C. O'Brien, R. F. Curl and R. E. Smalley, "C 60: buckminsterfullerene," *Nature*, vol. 318, pp. 162-163, 1985.

[2] A. G. MacDiarmid, ""Synthetic metals": A novel role for organic polymers (Nobel lecture)," *Angewandte Chemie International Edition*, vol. 40, pp. 2581-2590, 2001.

[3] A. Zarafshani, T. Bach, W. Wang and Chatwin C, "Multi-frequency response mesh phantom for validation of EIT system performance," *Reviewing at IOP: Physiological Measurement*, 2015.

[4] A. Zarafshani, N. Huber, N. Béqo, B. Tunstall, G. Sze, C. Chatwin and W. Wang, "A flexible low-cost, high-precision, single interface electrical impedance tomography system for breast cancer detection using FPGA," in *Journal of Physics: Conference Series*, 2010, pp. 012169.

[5] Xiaolin Zhang, Wei Wang, G. Sze, D. Barber and C. Chatwin, "An Image Reconstruction Algorithm for 3-D Electrical Impedance Mammography," *Medical Imaging, IEEE Transactions On*, vol. 33, pp. 2223-2241, 2014.

[6] T. Tallman, F. Semperlotti and K. Wang, "Enhanced health monitoring of fibrous composites with aligned carbon nanotube networks and electrical impedance tomography," in *SPIE Smart Structures and Materials Nondestructive Evaluation and Health Monitoring*, 2012, pp. 83480G-83480G-7.

[7] T. N. Tallman, S. Gungor, K. Wang and C. E. Bakis, "Damage detection via electrical impedance tomography in glass fiber/epoxy laminates with carbon black filler," *Structural Health Monitoring*, vol. 14, pp. 100-109, 2015.

[8] S. Gungor and C. E. Bakis, "Anisotropic networking of carbon black in glass/epoxy composites using electric field," *J. Composite Mater.*, pp. 0021998314521256, 2014.

[9] S. Gungor and C. E. Bakis, "Indentation damage detection in glass/epoxy composite laminates with electrically tailored conductive nanofiller," *J Intell Mater Syst Struct*, pp. 1045389X15577644, 2015.

[10] B. R. Loyola, L. Arronche, M. LaFord, V. La Saponara and K. J. Loh, "Evaluation of the damage detection characteristics of electrical impedance tomography," in *ASME 2013 Conference on Smart Materials, Adaptive Structures and Intelligent Systems*, 2013, pp. V002T05A017-V002T05A017.

[11] A. Todoroki, M. Tanaka and Y. Shimamura, "Measurement of orthotropic electric conductance of CFRP laminates and analysis of the effect on delamination monitoring with an electric resistance change method," *Composites Sci. Technol.*, vol. 62, pp. 619-628, 2002.

[12] R. Schueler, S. P. Joshi and K. Schulte, "Damage detection in CFRP by electrical conductivity mapping," *Composites Sci. Technol.*, vol. 61, pp. 921-930, 2001.

[13] W. Fan, H. Wang and Z. Cui, "Damage detection of CFRP composites using open electrical impedance tomography," in *2015 IEEE International Instrumentation and Measurement Technology Conference (I2MTC) Proceedings*, 2015, pp. 1377-1381.

[14] A. Hartov, R. A. Mazzarese, F. R. Reiss, T. E. Kerner, K. S. Osterman, D. B. Williams and K. D. Paulsen, "A multichannel continuously selectable multifrequency electrical impedance spectroscopy measurement system," *Biomedical Engineering, IEEE Transactions On*, vol. 47, pp. 49-58, 2000.

[15] A. Wilson, P. Milnes, A. Waterworth, R. Smallwood and B. Brown, "Mk3. 5: a modular, multi-frequency successor to the Mk3a EIS/EIT system," *Physiol. Meas.*, vol. 22, pp. 49, 2001.

[16] R. Bayford, "Bioimpedance tomography (electrical impedance tomography)," *Annu. Rev. Biomed. Eng.*, vol. 8, pp. 63-91, 2006.

[17] T. I. Oh, H. Wi, D. Y. Kim, P. J. Yoo and E. J. Woo, "A fully parallel multi-frequency EIT system with flexible electrode configuration: KHU Mark2," *Physiol. Meas.*, vol. 32, pp. 835, 2011.

[18] Data Sheet-ADG2128, "Analog switches multiplexers, I^2C CMOS, 8 X 12 analog switch array with dual/single supplies," Analog Devices, Tech. Rep. Rev. D, 2012b.

[19] R. A. Pease, "A comprehensive study of the Howland current pump," *National Semiconductor. January*, vol. 29, 2008.

[20] Data Sheet-AD844S, "Current conveyor, monolithic op amp, 60 MHz, 2000 V/ms, with current feedback amplifiers," Analog Devices;, Tech. Rep. REV. C, 2009.

[21] Data Sheet-AD8130, "Voltage measurement, low cost, 270 MHz differential receiver amplifier," Analog Devices, Tech. Rep. Rev. C, 2005b.

[22] Data Sheet-ADV3205, "Buffered analog crosspoints array, 60 MHz, G = +2, 16 ×16 buffered analog crosspoint switch," Analog Devices;, Tech. Rep. Rev 0, 2011.

[23] N. Polydorides and W. R. Lionheart, "A Matlab toolkit for three-dimensional electrical impedance tomography: a contribution to the Electrical Impedance and Diffuse Optical Reconstruction Software project," *Measurement Science and Technology*, vol. 13, pp. 1871, 2002.

[24] A. Adler and W. R. Lionheart, "Uses and abuses of EIDORS: an extensible software base for EIT," *Physiol. Meas.*, vol. 27, pp. S25, 2006.